Desalination and Water Treatment
www.deswater.com

doi: 10.1080/19443994.2013.842504

53 (2015) 785–793
January

Taylor & Francis
Taylor & Francis Group

Adsorption kinetics of the antibiotic ciprofloxacin on bentonite, activated carbon, zeolite, and pumice

Nevim Genç*, Esra Can Dogan

Faculty of Engineering, Department of Environmental Engineering, Kocaeli University, Kocaeli 41380, Turkey
Tel. +90 262 3033200; email: ngenc@kocaeli.edu.tr

Received 4 June 2013; Accepted 30 August 2013

ABSTRACT

This study analyzes ciprofloxacin (CIP) sorption by bentonite, activated carbon, zeolite, and pumice, which have been recently considered for their potential use in the adsorption of specific pollutants. Batch experiments were performed to investigate the adsorption kinetics between the adsorbents surfaces and CIP. Adsorption kinetics for adsorbents were well described by the pseudo-second kinetic model. The amount of CIP adsorbed by the adsorbents at equilibrium showed the following sequence: bentonite > activated carbon > zeolite > pumice. The adsorption thermodynamic parameters of the free energy change, the isosteric enthalpy change, and the entropy change for 22 °C were calculated. Thermodynamic of CIP adsorption shows that adsorption is the endothermic adsorption. The negative values of ΔG° for bentonite and activated carbon indicate the spontaneous nature of the adsorption. The positive value of ΔG° for zeolite and pumice indicates nonspontaneous nature of CIP adsorption. The positive entropy change indicated that the adsorption process was aided by increased randomness.

Keywords: Ciprofloxacin; Adsorption; Kinetic models; Thermodynamic

1. Introduction

Fluoroquinolo (FQ_s) are a class of potent synthetic antibiotics. Ciprofloxacin (CIP; $C_{17}H_{18}O_3N_3F$) is one of the most frequently prescribed human-use FQ_s in many countries [1]. CIP can be released into water sources due to incomplete metabolism in humans or coming from effluents of drug manufacturers. Degradation may not be the major process for the removal of compounds from wastewater treatment plants and hence the importance of sorption as an intervention technique [2]. In wastewater treatment, plants CIP is only partially eliminated, and residual amounts can reach surface water or groundwater [3]. A multiphase model used to predict the environmental concentrations is suitable for modelling the environmental fate of high water-soluble and low volatile organic compounds such as pharmaceuticals products [4].

CIP has a high aqueous solubility under various pH conditions and a higher stability in soil and wastewater systems. It was still often detected in the effluent of wastewater treatment plants [5]. The pK_a values for CIP are 5.90 ± 0.15 (for the carboxylic acid group) and 8.89 ± 0.11 for the basic-N-moiety, so it can exist as a cation, zwitterion and anion under typical soil and water pH conditions, as shown in Fig. 1 [6].

*Corresponding author.

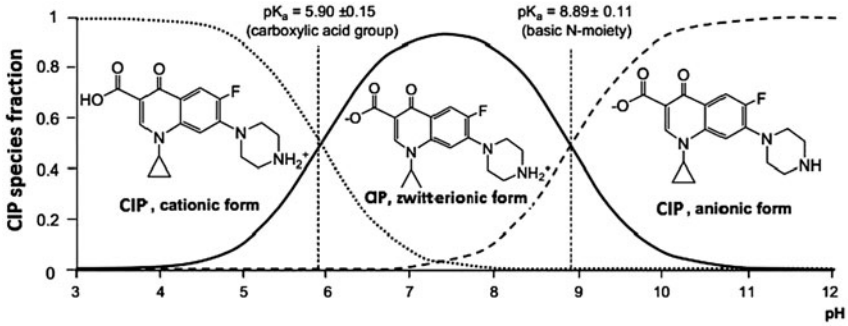

Fig. 1. Molecular structure of CIP and its ionic forms as a function of pH, pK_a values [6].

Several conventional processes, including adsorption, oxidation [7,8], photolytic and photocatalytic treatment [9,10], ozonation [11], oxidation by chlorination [12] and biological treatment [13,14] are commonly applied for the treatment of CIP/FQ_s in contaminated water. Among these processes, adsorption is a very attractive treatment method for the removal of CIP.

The sorption process can be described by the following consecutive steps [15]: (i) transport of solute in the bulk of the solution; (ii) diffusion of solute across the so-called liquid film surrounding sorbent particles; (iii) diffusion of solute in the liquid contained in the pores of sorbate particle and along the pore walls (intraparticle diffusion); (iv) adsorption and desorption of solute molecules on/from the sorbent surface. The overall sorption rate may mainly be controlled by any of these steps; a combined effect of a few steps is also possible. In many experimental sorption systems step (i) can be ignored. In order to determine the contribution of the remaining steps, numerous kinetic models have been used.

In acidic and neutral aqueous solutions, a stoichiometric exchange between CIP and interlayer cations yielded an high adsorption capacity. When solution pH was above its pK_{a2} (8.7), adsorption of CIP was greatly reduced due to the net repulsion between the negatively charged surfaces and the CIP anion [16].

Clay minerals are one of the most important adsorbents due to their high abundance, large specific surface area, negative charge, and hydrophilic surface. Bentonite is an inorganic clay mainly composed of montmorillonite. The widespread use of bentonite can be attributed to its physical and chemical properties such as small particle size, high porosity, large surface area and high cation-exchange capacity. The bentonite has excellent adsorption capacity and adsorption ability [17]. It contains exchangeable inorganic cations on the internal and external surfaces of montmorillonite that upon replacement with organic cations enhance the adsorption capacity for the removal of organic pollutants [18]. Bentonite has been widely used in studies of adsorption of pollutants from wastewater [17–21]. Previous research on interactions between CIP and clay minerals were focused mainly on swelling clays as they have a much higher CIP adsorption capacity. The dominant mechanism of CIP adsorption on clay is cation exchange. FQ molecules appear to be beter suited for cation exchange than for cation bridging or surface complexation.

When CIP was sorbed on montmorillonite at pH 4.5, cation exchange between the protonated heterocyclic N atom of CIP^+ and the negatively charged montmorillonite surface should be the main sorption mechanism on montmorillonite. At pH 7.0, the carboxylate anion was the dominant species. CIP^- was sorbed on montmorillonite mainly through the interaction of its carboxylic group [22].

To date, several reports related to the adsorption of CIP to natural materials or components of natural materials have been published (activated carbon [6] AC; activated charcoal and talc [23]; montmorillonite [24,25]; soil [26–28]; 2:1 dioctahedral clay minerals [29]; kaolinite [30]; modified coal fly ash [31]; aerobically digested biosolid [32]; sawdust [33], date palm leaflets [34]; birnessite, a layered manganese oxide [5]; (Fe_30_4/C) a new magnetic mesoporous carbon composite [35]; Chitosan/Zn (II), Chitosan/Fe (III), Chitosan/Fe(II) microparticles [36]; aluminum and hydrous oxides [37]; nano-sized magnetite [38]).

The objective of this research is to investigate the capability of bentonite, activated carbon, zeolite, and pumice for the adsorption of CIP from aqueous solution. On the basis of batch adsorption experiments, kinetic models to predict the CIP removal efficiency of a low cost adsorbent used is applied. In this paper, the popular mathematical formulae are presented, extensively applied for correlating the kinetic data, for example. the pseudo-first, pseudo-second, Elovich, and intraparticle diffusion equations are presented.

These formulae have usually been associated with the surface-reaction kinetic step as controlling the sorption rate. Thermodynamic studies were also performed in order to explain the adsorption mechanism.

2. Models overview

Numerous kinetic models have been compared to predict the behaviour of the experimental data. Many simple, compact formulas, such as the pseudo-first, pseudo-second, Elovich equations, and intraparticle diffusion model have been applied for correlating kinetic data measured in many different systems. At present, the most popular are the pseudo-first- and the pseudo-second-order equations. As noted by Liu and Liu (2008) [39], these two expressions are commonly "employed in parallel, an done is often claimed to be better than another according to marginal difference in correlation coefficient."

The pseudo-first-order equation has the following formulation Eq. (1) [15]:

$$\ln(q_e - q_t) = \ln q_e - k_1 t \quad (1)$$

where q_t (mg CIP/g adsorbent) is the concentration of CIP in the solid phase, q_e (mg CIP/g adsorbent) is the equilibrium concentrations of CIP in the solid phase, k_1 (1/min) is the observed rate constant of the pseudo-first-order model, and t (min) is time. The values of q_e and k_1 parameters are usually determined by applying the commonly accepted linear regression procedure. In the first-order kinetic model, by plotting the values of $\ln(q_e - q_t)$ vs. t may give a linear relationship that k_1, and q_e values can be determined from the slope and intercept of the obtained line, respectively [40]. The k_1 parameter decides how fast the equilibrium in the system can be reached. The value of k_1 parameter can be both dependent and independent of the applied operating conditions [15]. k_1 is a combination of adsorption and desorption rate constants and is not the intrinsic adsorption rate constant [41].

The most commonly applied form of the pseudo-second-order equation can be written in Eq. (2):

$$\frac{t}{q_t} = \frac{1}{k_2 q_e^2} + \frac{1}{q_e} t \quad (2)$$

where k_2 (g adsorbent/mg CIP min) is a constant. The value of k_2 strongly depends on the applied operating conditions. The k_2 constant value is usually strongly dependent on the applied initial solute concentration. k_2 is a complex function of the initial concentration of solute [41]. It decreases with the increasing C_{in} as a rule. Only very few systems for which k_2 is C_{in}-independent or increases with the C_{in} value have been reported. Usually, the higher value of q_e is correlated with the higher value of k_2 [15].

The pseudo-second-order model is based on the assumption that the rate-limiting step may be chemical adsorption involving valence forces through sharing or exchange of electrons between adsorbent and adsorbate. It is assumed that the sorption capacity is proportional to the number of active sites occupied on the adsorbent [31].

The Elovich equation is the rate equation, its integral form reads Eq. (3):

$$q_t = \frac{1}{\beta}\ln(\alpha\beta) + \frac{1}{\beta}\ln(t) \quad (3)$$

in which α is the initial adsorption rate (mg/g min), and β is the adsorption constant (g/mg). If experimental data fit the Elovich model, a plot of q_t vs. $\ln(t)$ should yield a linear relationship with a slope of $1/\beta$ and an intercept of $(1/\beta)\ln(\alpha t)$. A decrease in β and/or an increase in α would increase reaction rate [42]. The Elovich equation can be successfully employed to describe the adsorption kinetics of ion exchange system, so it could be deduced that the adsorption process is a chemical process, especially an ion-exchange process [43].

Intraparticle diffusion model based on diffusive mass transfer that adsorption rate expressed in terms of the square root of time is given (Eq. 4) [40].

$$q_t = k_{diff} t^{0.5} + C \quad (4)$$

k_{diff} (mg/g $\text{min}^{0.5}$) is the intraparticle diffusion rate constant and C is a constant related to the thickness of the boundary layer, which is in direct ratio to the effect of the boundary layer. The value of k_{diff} and C were calculated from the slope and intercept of the plot of q_t vs. $t^{0.5}$. Generally, the plot of q_t against $t^{0.5}$ may show a multilinearity, and this indicated that the adsorption processes contained two or more steps. The adsorption of a solute from solution by porous adsorbents is essentially relevant to three consecutive steps. The external surface adsorption or the instantaneous adsorption is the first step. The second step is gradual adsorption stage where intraparticle diffusion is rate limiting. The third step is the final equilibrium stage where intraparticle diffusion starts to slow down due to the extremely low adsorbate concentrations that remain in the solutions. If the line passed through the origin, the intraparticle diffusion would be the sole rate-limiting step. If the line did not pass through the origin, it implied that

intraparticle diffusion was not the sole rate control step, and other processes may control the adsorption rate [43].

3. Materials and methods

3.1. Materials

The minerals used for the experiments are zeolite, bentonite, pumice, and activated carbon. Mineral samples were air-dried and passed through a sieve to ensure the material uniformity. The bentonite used observed from Çankırı-Turkey. Particle size is < 0.6 mm. Chemical structure natural zeolite (Clinoptiolite) obtained from Rota Mining i.e. Turkey is $(Ca, K_2, Na_2, Mg)_4Al_8Si_{40}O_{96}.24H_2O$. Total CEC is 1.5–2.1 meq/g and particle size is < 700 micron. BET surface area of powder-activated carbon used is 990 m^2/g (ZAG, CAS No: 7,440–44-0). Pumice is approximately composed of 75% SiO_2 and has amorphous and pore structure. It's specific density is 1–2 g/cm^3. CIP hydrochloride with purity higher than 99% was obtained from SANOVEL. Limit of fluoroquinolonic acid is less than 0.2% (w/w). Particle size distriubution on 20 ASTM is 0.24%.

3.2. Batch CIP hydrochloride adsorption experiments

For a kinetic study, a series of 50 mL of CIP solution at different initial concentrations (20, 25, 30, and 40 mg/L) with 0.0125 g of adsorbent were shaked by shaking equipment at 22°C temperature under 150 rpm. The flasks were then taken out of shaking equipment at 5, 10, 20, 30, 40, 50, and 60 min time intervals. The initial pH values of the CIP solutions were not adjusted.

3.3. Analysis

The concentrations of CIP in the residual solutions were analyzed by means of the UV spectrometer (Hach-Lange DR 5000). The concentration of CIP was analyzed at the maximum wavelength. The calibration curve was established with 10 standards between 0 and 5 mg/L with the coefficient of determination ($R^2 = 0.9998$). The adsorption capacities were calculated according to a mass balance of CIP in the solutions and were represented in units of miligrams of CIP per gram of adsorbent. The adsorption capacities at equilibrium were computed according to Eq. (5):

$$q_e = \frac{(C_o - C_e)V}{m} \quad (5)$$

where q_e and C_e are the amount adsorbed (mg/ g) and the residual concentration (mg/ L) at equilibrium, respectively; C_o is the initial concentration of CIP (mg/ L); V and m are the volume of CIP solution (L) and the mass of adsorbent used (g), respectively.

4. Results and discussion

4.1. Sorption kinetics

Clay minerals and pumice, evaluated as an alternative adsorbents for CIP removal, are a vastly available materials in Turkey. CIP adsorption on adsorbents surfaces has been described in terms of cation exchange in the interlayer and surface complexation. The protonated amine groups and the carboxylic groups of the CIP molecules were responsible for the electrostatic attraction and hydrogen bonding to the external and internal surfaces of the clay minerals [29].

Pumice has a skeleton that allows ions and molecules to reside and move within the overall framework. The structure contains open channels that allow water and ions to travel into and out of the crystal structure.

Activated carbon has the highest surface area. Since CIP has an almost planar configuration, in principle, it should be able to penetrate into the pores of AC. As the micropores are normally "slit" shaped, the molecule should be able to enter "sideways" [6].

A possible explanation for the better performance of AC can lie in the influence of the electrostatic forces. In this case, it might be that the adsorption is not only π–π, but that there are also some interactions with the functional groups. At pH 5 (pH of water, at which the adsorption experiments were carried out), the cationic protonated form of CIP is more abundant. The surface of activated carbon contains carboxylic acid groups and is negatively charged at the experimental pH around 5 ($pH > pH_{PZC}$), thus attracting CIP [6].

In this study, the solution pH for the kinetic experiments was about 5.5 below the pK_{a1} value of CIP. Thus, CIP was in its cationic form. FQ molecules were speculated to better suit for cation exchange (via the ammonium group) than for cation bridging or surface complexation (via the carboxyl group on the zwitterion) [24].

Adsorption kinetic studies provide one of the important methods for illustrating the efficiency of an adsorption process and for estimating the residual time necessary for the whole process. The kinetics of CIP adsorption on bentonite, activated carbon, zeolite and pumice were investigated by changing the contact

time from 0 to 60 min. Fig. 2 shows that the adsorption capacity of CIP increased with time, to attain a maximum value and finally reach equilibrium. The curves also show that the adsorption capacity of CIP on bentonite is higher than that of activated carbon, zeolite, and pumice. For bentonite, activated carbon, and zeolite, adsorption CIP on adsorbents were decreased with increasing initial CIP concentration. The highest removal efficiency was calculated as 91, 87, and 51% for bentonite, activated carbon, and zeolite, respectively, at 20 mg/L initial concentrations. For pumice, the highest removal efficiency was calculated as 25% at initial concentration of 40 mg/L. The kinetic parameters calculated from models were listed in Table 1.

It was shown that the second-order model fits better to most of the adsorption data, since the line corresponding to the model fitting is closer to the experimental points than that form the first-order model. R^2 values are higher in the case of second-order fitting. If the intercept does not equal to experimental q_e value, it can be considered that the reaction is not likely to be a first-order reaction even this plot has a high correlation coefficient [40]. For all adsorbents, experimental data not fit to first-order kinetic due to $q_{e,calc}$ values calculated by first-order kinetic are not equal to $q_{e,exp}$.

For the all initial concentration of CIP, the equilibrium concentration in solid phase increases in the order of bentonite > activated carbon > zeolite > pumice. Generally, the rate constant decreases for larger concentrations due to limited adsorption sites on adsorbents. For bentonite, when initial concentration is increase from 20 to 40 mg/L, k_2 value is decrease from 18.3. to $5.18.10^{-3}$ (g/mg min).

When k_2 value is relatively high, the time required to reach an equilibrium state by the system is relatively short; an opposite situation occurs for small k_2 [15]. According to Table 1, pumice is adsorbent that the time required to reach an equilibrium is shorter. k_2 value from the present study was compared with other adsorbents in previous studies (Table 2).

The experimental data are tested by the intraparticle diffusion model. The plot of q_t vs. $t^{0.5}$ for CIP on adsorbents was shown that the experimental data points showed sole linear sections, which indicates one step in adsorption process. Intraparticle diffusion analysis demonstrates that CIP diffuses higher among bentonite, activated carbon, and zeolite particles than modified coal ash fly (0.0324 mg/g $min^{0.5}$)[31] and chemically prepared carbon date palm leaflets (0.267 mg/g $min^{0.5}$ for wet adsorbent, 0.211 mg/g $min^{0.5}$ for dry adsorbent) [34].

According to Elovich model analysis, the initial adsorption rate for bentonite was 18.10^5 to 60.10^{12} mg/g min, much faster than activated carbon, zeolite, and pumice.

4.2. Thermodynamics of CIP adsorption

The relationship between the CIP distribution coefficient (K_d) and free energy (ΔG° J/mol) of adsorption (Eq. (6)) is:

$$\Delta G^\circ = -RT \ln K_d \quad (6)$$

where ΔG° is the standard free energy change, R (8.314 J/mol K) is the gas constant, and T is the reaction temperature in K. The distribution coefficient

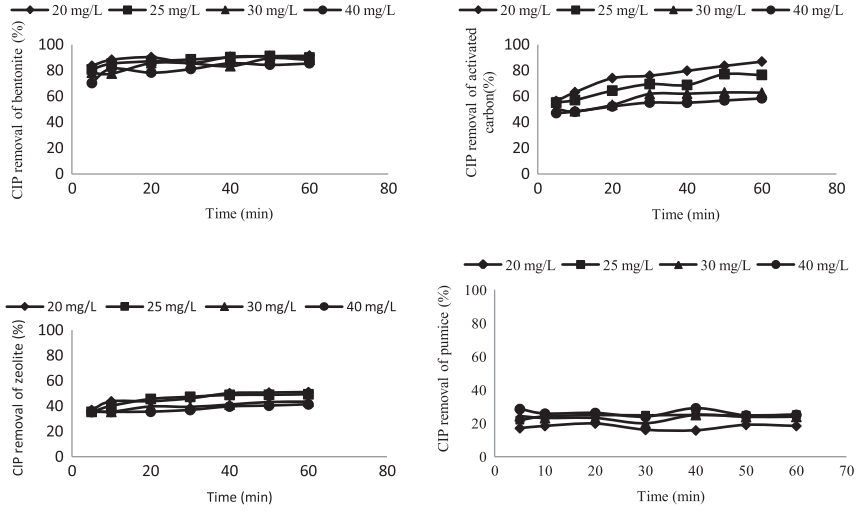

Fig. 2. Adsorption rate curves of CIP onto the four adsorbents.

Table 1
The kinetic parameters for the adsorption of CIP on adsorbents

Adsorbent	C_{in} (mg/L)	First-order kinetic				Second-order kinetic			Elovic			Intra particle difussion		
		$q_{e,exp}$ (mg/g)	$q_{e,calc}$ (mg/g)	k_1 (1/min)	R^2	$q_{e,calc}$ (mg/g)	k_2 (g/mg min)	R^2	α (mg/g min)	β (g/mg)	R^2	k_{dif} (mg/g $min^{0.5}$)	C	R^2
	20	69.48	34.75	0.0534	0.9568	72.99	3.07×10^{-3}	0.9968	193.13	0.104	0.9884	4.2656	37.12	0.9725
Activated	25	77.15	42.99	0.0648	0.8767	81.97	3.01×10^{-3}	0.9933	570.40	0.109	0.9265	4.1704	45.141	0.9557
carbon	30	75.51	28.80	0.0752	0.9204	79.37	2.99×10^{-3}	0.9978	2,480	0.129	0.8354	3.4927	50.591	0.8592
	40	93.49	26.80	0.0495	0.9523	95.24	3.25×10^{-3}	0.9989	24,960	0.132	0.9609	3.3608	67.145	0.9871
	20	73.14	4.78	0.0387	0.4928	73.53	18.3×10^{-3}	0.9989	60.10^{12}	0.482	0.6028	0.9031	66.216	0.5724
Bentonite	25	91.06	9.38	0.0434	0.8541	91.74	13.8×10^{-3}	0.9998	1085×10^{6}	0.258	0.9481	1.6581	78.91	0.8709
	30	106.85	17.35	0.0460	0.7787	107.53	7.33×10^{-3}	0.9981	385×10^{5}	0.189	0.7804	2.3545	88.388	0.7726
	40	137.10	28.4	0.0658	0.8178	138.89	5.18×10^{-3}	0.9999	18×10^{5}	0.119	0.7681	3.6062	110.72	0.7107
	20	40.70	16.84	0.0653	0.9098	42.73	7.45×10^{-3}	0.9973	826.47	0.228	0.9293	1.9358	26.64	0.9106
Zeolite	25	49.21	20.73	0.0837	0.9788	51.30	7.71×10^{-3}	0.9999	592.53	0.173	0.9681	2.474	32.08	0.888
	30	52.00	15.94	0.0573	0.8003	53.48	7.70×10^{-3}	0.9975	63,370	0.271	0.8469	1.7101	38.715	0.9107
	40	65.93	15.75	0.0415	0.8565	67.57	5.95×10^{-3}	0.9965	646,350	0.252	0.7614	1.9021	50.35	0.8763
	20	15.91	2.29	0.0098	0.1099	14.53	$86.38. 10^{-3}$	0.9771	–	–	0.0016	–	–	0.0012
Pumice	25	25.21	1.59	0.0442	0.485	25.32	$72.91. 10^{-3}$	0.9998	–	0.923	0.7438	0.4363	22.16	0.6054
	30	29.97	1.93	0.0002	6E–05	39	$30.76. 10^{-3}$	0.9859	–	–	0.0018	–	–	0.0021
	40	46.41	2.07	−0.025	0.3918	40.16	$-38.75. 10^{-3}$	0.9883	–	–	0.1875	–	–	0.1561

(–): not calculated.

Table 2
k_2 value of different adsorbents used for the removal of CIP

Adsorbent	k_2 (g/mg min)	References
Kaolinite	855×10^{-3}	[30]
Montmorillonite	133.3×10^{-3}	[29]
	2.33×10^{-3}	[24]
Rectorite	3.33×10^{-3}	[29]
Illite	5×10^{-3}	[29]
Modified coal fly ash	2.07	[31]
Chemically prepared wet and dry carbon	0.2×10^{-3} and 0.18×10^{-3}	[34]
Birnessite	322×10^{-3}	[5]
Molecularly imprinted polymer and non-imprinted polymer	1.381 and 0.472	[1]

Table 3
Calculated thermodynamic parameters for CIP adsorption on adsorbents for 22°C

C_{in} (mg/L)	Bentonite			Activated carbon			Zeolite			Pumice		
	ΔG°	ΔH°	ΔS°	ΔG°	ΔH°	ΔS°	ΔG°	ΔH°	ΔS°	ΔG°	ΔH°	ΔS°
20	−5,810	7,130	43.86	−4,630	7,000	39.43	−96.19	5,603	19.32	3,419	3,384	−0.12
25	−5,370	7,635	44.08	−2,900	7,240	34.37	74.70	6,158	20.62	2,668	4,514	6.26
30	−4,930	8,034	43.94	−1,270	7,199	28.71	673	6,276	19	2,704	4,941	7.58
40	−4,340	8,662	44.07	−843	7,739	29.08	875	6,869	20.32	2,199	6,009	12.92

for the adsorption process, K_d, calculated with Eq. (7), was evaluated at 22°C [44].

$$K_d = \frac{X_e}{C_{in} - X_e} \tag{7}$$

where X_e is the concentration of solute adsorbed on the adsorbate at equilibrium (mg/L); C_{in} the initial CIP concentration (mg/L). ΔH° (J/mol) and ΔS° (J/mol K) according to Eqs. (8) and (9) are calculated [45].

$$\log\left(\frac{1}{C_e}\right) = \log K_d + \left(\frac{-\Delta H^\circ}{2.303RT}\right) \tag{8}$$

$$\Delta S^\circ = \frac{\Delta H^\circ - \Delta G^\circ}{T} \tag{9}$$

where C_e is the equilibrium concentration of solution, ΔH is the isosteric enthalpy change, ΔS is the entropy change. Calculated thermodynamic parameters are presented in Table 3.

Table 3 shows the adsorption of CIP on the four adsorbents are all the endothermic adsorption process or vice versa, which is suggested by the positive values of the enthalpy changes. Entropy has been defined as the degree of chaos of a system. The positive value of ΔS suggests that some structural changes occur on the adsorbent, and the randomness at the solid/liquid interface in the adsorption system increases during the adsorption process [46].

The negative value of ΔG° indicates a decrease in Gibbs free energy, which verifies the feasibility and spontaneity of the adsorption process with a high affinity of CIP on adsorbents [42]. According to Fig. 3, the affinity to CIP of adsorbents is the order of bentonite > activated carbon > zeolite > pumice. The calculated ΔG° values for bentonite, zeolite, activated carbon, and pumice can be compared with −12,000 to

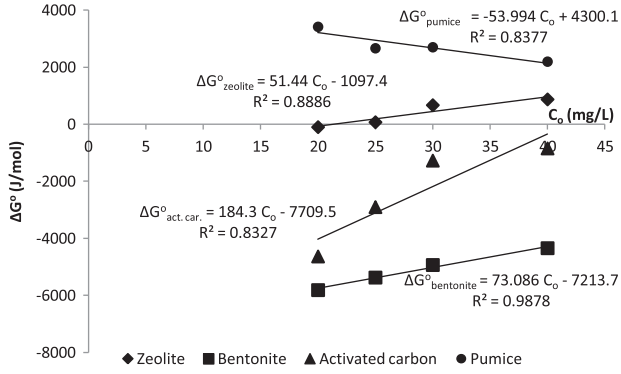

Fig. 3. Free energy of adsorption of CIP as a function of initial CIP concentration.

-19,000 J/mol for CIP adsorption on kaolinite at initial concentrations 331.4 mg/L-662.8 mg/L [30]. ΔG° changes of CIP on modified coal fly ash is −2,824 to −5,396 J/mol for 30 °C [31].

5. Conclusions

The adsorption of CIP from aqueous solutions onto bentonite, activated carbon, zeolite, and pumice has been studied. Many simple, compact formulas such as the pseudo-first, pseudo-second, Elovich equations and intraparticle diffusion have been applied for correlating kinetic data measured in batch CIP adsorption experiments. The following conclusions may be drawn:

The experimental data showed a high degree of nonlinearity and poor correlation coefficient for the pseudo-first-order, Elovich, intraparticle diffusion models. The best-fit model was selected based on the linear regression correlation coefficient values (R^2). Pseudo-second-order kinetic model gives a straight line with a high correlation coefficient. The values of R^2 and closeness of experimental and theoretical adsorption capacity value show the applicability of the second-order model to explain and interpret the experimental data. Adsorption capacity value for bentonite is quite significant as compared with other adsorbents and value of adsorption capacity for bentonite is the highest.

Although activated carbon are well-known "universal" adsorbents and present unique advantages due to their low cost, high adsorption capacity and easy disposal, the CIP adsorption capacity on bentonite was much higher compared with that on activated carbon, pumice, and zeolite. On the other hand, it may serve as an environmental sink for cationic drug such as CIP. The highest removal efficiencies were calculated as 91, 87, and 51% for bentonite, activated carbon, and zeolite, respectively, at 20 mg/L initial concentrations. For pumice, the highest removal efficiency was calculated as 25% at initial concentration of 40 mg/L. For the all initial concentration of CIP, the equilibrium concentration in solid phase and the affinity to CIP of adsorbents increases in the order of bentonite > activated carbon > zeolite > pumice.

Thermodynamic of CIP adsorption shows that adsorption is the endothermic adsorption. The negative values of ΔG° for bentonite and activated carbon indicate the spontaneous nature of the adsorption. The positive value of ΔG° for zeolite and pumice indicates nonspontaneous nature of CIP adsorption. The positive entropy change indicated that the adsorption process was aided by increased randomness.

References

[1] X. Zhang, X. Gao, P. Huo, Y. Yan, Selective adsorption of micro ciprofloxacin by molecularly imprinted functionalized polymers appended onto ZnS, Environ. Technol. 33(17) (2012) 2019–2025.
[2] L.J.M. Githinji, M.K. Musey, R.O. Ankumah, Evaluation of the fate of ciprofloxacin and amoxicillin in domestic wastewater, Water Air Soil Pollut. 219 (2011) 191–201.
[3] S.A.C. Carabineiro, T. Thavorn-Amornsri, M.F.R. Pereira, J.L. Figueiredo, Adsorption of ciprofloxacin on surface-modified carbon materials, Water Res. 45 (2011) 4583–4591.
[4] X. Domènech, M. Ribera, J. Peral, Assessment of pharmaceuticals fate in a model environment, Water Air Soil Pollut. 218 (2011) 413–422.
[5] W.T. Jiang, P.H. Chang, Y.S. Wang, Y. Tsai, J.S. Jean, Z. Li, K. Krukowski, Removal of ciprofloxacin from water by birnessite, J. Hazard. Mater. 250–251 (2013) 362–369.
[6] S.A.C. Carabineiro, T. Thavorn-amornsri, M.F.R. Pereira, P. Serp, J.L. Figueiredo, Comparison between activated carbon, carbon xerogeland carbon nanotubes for the adsorption of the antibiotic ciprofloxacin, Catal. Today 186 (2012) 29–34.
[7] X.A. Xiao, X. Zeng, A.T. Lemley, Species-dependent degradation of ciprofloxacin in a membrane anodic fenton system, J. Agric. Food Chem. 58(18) (2010) 10169–10175.
[8] X. Xiao, S.P. Sun, M. McBride, A. Lemley, Degradation of ciprofloxacin by cryptomelane-type manganese (III/IV) oxides, Environ. Sci. Pollut. Res. 20(1) (2013) 10–21.
[9] W.H. Li, C.S. Guo, S. Su, J. Xu, Photodegradation of four fluoroquinolone compounds by titanium dioxide under simulated solar light irradiation, J. Chem. Technol. Biotechnol. 87(5) (2012) 643–650.
[10] M.I. Vasquez, E. Hapeshi, D. Fatta-Kassinos, K. Kuemmerer, Biodegradation potential of ofloxacin and its resulting transformation products during photolytic and photocatalytic treatment, Environ. Sci. Pollut. Res. 20(3) (2013) 1302–1309.
[11] D. Nasuhoglu, A. Rodayan, D. Berk, V. Yargeau, Removal of the antibiotic levofloxacin (LEVO) in water by ozonation and TiO_2 photocatalysis, Chem. Eng. J. 189 (2012) 41–48.
[12] B. Li, T. Zhang, PH significantly affects removal of trace antibiotics in chlorination of municipal wastewater, Water Res. 46 (11) (2012) 3703–3713.
[13] B. Li, T. Zhang, Biodegradation and adsorption of antibiotics in the activated sludge process, Environ. Sci. Technol. 44(9) (2010) 3468–3473.
[14] N. Dorival-Garcia, A. Zafra-Gomez, A. Navalon, J. Gonzalez, J.L. Wilchez, Removal of quinolone antibiotics from wastewaters by sorption and biological degradation in laboratory-scale membrane bioreactors, Sci. Total Environ. 442 (2013) 317–328.
[15] W. Plazinski, W. Rudzinski, A. Plazinska, Theoretical models of sorption kinetics including a surface reaction mechanism: A review, Adv. Colloid Interface Sci. 152 (2009) 2–13.
[16] C.J. Wang, Z. Li, W.T. Jiang, J.S. Jean, C.C. Liu, Cation exchange interaction between antibiotic ciprofloxacin and montmorillonite, J. Hazard. Mater. 183 (2010) 309–314.
[17] D. Doulia, C.H. Leodopoloud, K. Gimouhopoulos, F. Rigas, Adsorption of humic acid on acid-activated Greek bentonite, J. Colloid and Interface Sci. 340 (2009) 131–141.
[18] M. Salman, M. Athar, U. Shafique, R. Rehman, S. Ameer, S.Z. Ali, M. Azeem, Removal of formaldehyde from aqueous solution by adsorption on kaolin and bentonite: A comparative study, Turkish J. Eng. Env. Sci. 36 (2012) 263–270.
[19] M. Akçay, G. Akçay, The removal of phenolic compounds from aqueous solutions by organophilic bentonite, J. Hazard. Mater. 113 (2004) 189–193.
[20] A.S. Özcan, B. Erdem, A. Özcan, Adsorption of acid blue 193 from aqueous solutions onto BTMA-Bentonite, Colloid Surf. A: Physicochem Eng. Aspects 266 (2005) 73–81.
[21] J.G. Meneguin, G.R. Luz, I.C. Ostroski, M.A. Barros, M.L. Gimenes, Removal of heavy metals in K-bentonite clay, Chem. Eng. Trans. 24 (2011) 787–792.

[22] Z. Pei, X.Q. Shan, J. Kong, B. Wen, G. Owens, Coadsorption of ciprofloxacin and Cu (II) on montmorillonite and kaolinite as affected by solution pH, Environ. Sci. Technol. 44 (2010) 3.
[23] E.C. Ibezim, S.I. Ofoefule, C.N.E. Ejeahalaka, O.E. Orisakwe, In vitro adsorption of ciprofloxacin on activated charcoal and talc, Am. J. Terapeutics 6(4) (1999) 199–201.
[24] Q. Wu, Z. Li, H. Hong, K. Yin, L. Tie, Adsorption and intercalation of ciprofloxacin on montmoriionite, Appl. Clay Sci. 50 (2010) 204–211.
[25] W. Qinfeng, L. Zhaohui, H. Hanlie, Influenceof types and charges of exchangeable cations on ciprofloxacin sorption by montmorillonite, J. Wuhan University Technol. Mater. Sci. 27 (3) (2012) 516–522.
[26] A.J. Carrasquillo, G.L. Bruland, A.A. Mackay, D. Vasudevan, Sorption of ciprofloxacin and oxytetracycline zwitterions to soils and soil materials: Influence of compound structure, Environ. Sci. Technol. 42 (2008) 7634–7642.
[27] D. Vasudevan, G.L. Bruland, B.S. Torrance, V.G. Upchurch, A.A. MacKay, pH-dependent ciprofloxacin sorption to soil: Interaction mechanisms and soil factors influencing sorption, Geoderma 151 (2009) 68–76.
[28] J.L. Conkle, C. Lattao, J.R. White, R.L. Cook, Competitive sorption and desorption behavior for three fluoroquinolone antibiotics in a wastewater treatment wetland soil, Chemosphere 80(11) (2010) 1353–1359.
[29] C.J. Wang, Z. Li, W.T. Jiang, Adsorption of ciprofloxacin on 2:1 dioctahedral clay minerals, Appl. Clay Sci. 53 (2011) 723–728.
[30] Z. Li, H. Hong, L. Liao, C.J. Ackley, L.A. Schulz, R.A. MacDonald, A.L. Mihelich, S.M. Emard, A mechanistic study of ciprofloxacin removal by kaolinite, Colloids Surf., B 88 (2011) 339–344.
[31] C.L. Zhang, G.L. Qiao, F. Zhao, Y. Wang, Thermodynamic and kinetic parameters of ciprofloxacin adsorption onto modified coal fly ash from aqueous solution, J. Mol. Liq. 163 (2011) 53–56.
[32] C. Wu, A.L. Spongberg, J.D. Witter, Sorptionand biodegradation of selected antibiotics in biosolids, J. Environ. Sci. Health., Part A 44 (2009) 454–461.
[33] S.K. Bajpai, M. Bajpai, N. Rai, Sorptive removal of ciprofloxacin hydrochloride from simulated wastewater using sawdust: Kinetic study and effect of pH, Water SA 38(5) (2012) 673–682.
[34] E.S.I. El-Shafey, H. Al-Lawati, A.S. Al-Sumri, Ciprofloxacin adsorption from aqueous solution onto chemically prepared carbon from date palm leaflets, J. Environ. Sci. 24(9) (2012) 1579–1586.
[35] S. Shi, Y.W. Fan, Y.M. Huang, Facile low temperature hydrothermal synthesis of magnetic mesoporous carbon nanocomposite for adsorption removal of ciprofloxacin antibiotics, Ind. Eng. Chem. Res. 52(7) (2013) 2604–2612.
[36] F. Reynaud, N. Tsapis, M. Deyme, T.G. Vasconcelos, C. Gueutin, S.S. Guterres, A.R. Pohlmann, E. Fattal, Spray-dried chitosan-metal microparticles for ciprofloxacin adsorption: Kinetic and equilibrium studies, Soft Matter 7(16) (2011) 7304–7312.
[37] C. Gu, K.G. Karthikeyan, Sorption of the antimicrobial ciprofloxacin to aluminum and iron hydrous oxides, Environ. Sci. Technol. 39 (2005) 9166–9173.
[38] S. Rakshit, D. Sarkar, E.J. Elzinga, P. Punamiya, R. Datta, Mechanisms of ciprofloxacin removal by nano-sized magnetite, J. Hazard. Mater. 246–247 (2013) 221–226.
[39] Y. Liu, Y.J. Liu, Biosorption isotherms, kinetics and thermodynamics, Sep. Purif. Technol. 61 (2008) 229–242.
[40] M. Ghaedi, S.N. Kokhdan, Oxidized multiwalled carbon nanotubes for the removal of methyl red (MR): Kinetics and equilibrium study, Desalin. Water Treat. 49 (2012) 317–325.
[41] S. Azizian, Kinetic models of sorption: A theoretical analysis, J. Colloid Interface Sci. 276 (2004) 47–52.
[42] O. Moradi, A. Fakhri, S. Adami, S. Adami, Isotherm, thermodynamic, kinetics, and adsorption mechanism studies of Ethidium bromide by single-walled carbon nanotube and carboxylate group functionalized single-walled carbon nanotube, J. Colloid Interface Sci. 395 (2013) 224–229.
[43] W. Zou, H. Bai, S. Gao, Competitive adsorption of neutral red and Cu^{2+} onto pyrolytic char: Isotherm and kinetic study, J. Chem. Eng. Data 57 (2012) 2792–2801.
[44] A. Eser, V.N. Tirtom, T. Aydemir, S. Becerik, A. Dinçer, Removal of nickel (II) ions by histidine modified chitosan beads, Chem. Eng. J. 210 (2012) 590–596.
[45] W. Hai-ling, F. Zheng-hao, C. Jin-long, Z. Quan-xing, X.U. Yan-long, Adsorption thermodynamics and kinetic investigation of aromatic amphoteric compounds onto different polymeric adsorbents, J. Environ. Sci. 19 (2007) 1298–1304.
[46] J. He, S. Hong, L. Zhang, F. Gan, Y.S. Ho, Equilibrium and thermodynamic parameters of adsorption of methylene blue onto rectorite, Fresenius Environ. Bull. 19(11a) (2010) 2651–2656.